

EXPERIMENTAL RESULTS ON SAND TRANSPORT UNDER WAVES IN LARGE-SCALE WAVE FLUME

DANG HUU CHUNG

Institute of Mechanics, NCST of Vietnam

ABSTRACT. The paper presents some results of a study based on the experiment carried out in Delta Flume of Delft Hydraulics. The analysis of time-series of sand concentration and velocity are implemented for regular and irregular waves with different conditions on wave and grain size. From measured concentrations and velocities the suspended transport components are calculated and some interesting information is obtained. At the same time some formulae for calculations of suspended sediment transport have been proposed and verified. A general evaluation on the total sediment transport rate over the water depth has been given on the basis of incorporating measurement, extrapolation and bedload prediction.

1. Introduction

Sediment transport is a very complicated natural process and so far it is not fully understood yet. Therefore every different attempt to achieve knowledge on this phenomenon in some measure is always encouraged. The current-related transport component involves the convective sand transport carried by the mean currents such as tide, wind and wave-driven currents in the presence of short (high-frequency) surface waves acting as stirring agents. The wave-related sand transport is herein defined as the transport of sand particles by the oscillating fluid motion due to the high-frequency waves. The current-related transport over rippled beds has been studied in considerable detail (Van Rijn et al., 1993; Van Rijn and Havinga, 1995), but the wave-related transport is less well known. The wave-related transport over a flat bed has been studied in more detail based on numerous experiments in wave tunnels (see for overview: Ribberink, 1998).

Within this purpose the paper presents some results on the analysis of time series of concentration and 2DH velocity components under regular and irregular waves that were measured from the Delta Flume at the laboratory by the Dutch researchers of Delft Hydraulics in 1998. In this way, the different components of sediment transport are evaluated. At the same time on the basis of the analysis some remarks and methods for calculation of wave-related suspended sand transport have been proposed. By using extrapolation and bedload transport a general

evaluation on the relative importance of transport components in three layers has been given. A new acoustical instrument, Acoustical Sand Transport Meter (ASTM) was used for measuring both the velocity and the suspended sediment concentration simultaneously at five elevations above the bed.

The tests in the Delta Flume were carried out as a part of the European Large Installation Plan (LIP) with modern equipment. Therefore, in order to supply the detail of the experiment as well as the physical sense of measured data, their description and setting up are also presented.

2. Experimental design

2.1. Description of instruments

The experiments were carried out in the Delta Flume of Delft Hydraulics. This is a large-scale flume that has a total length of 233 meters, a depth of 7 meters and a width of 5 meters. On the bed a sand layer of 0.5 m was placed over a length of about 40 m (see Fig. 1). Regular and irregular waves were generated by a piston activated wave board on one side of the flume. The instruments for measurement were mounted in a tripod, which was placed on the sand bed at location $x = 125$ m. For each test the instruments were operated for about 15 minutes to sample over a representative wave record.

The following instruments were used in the flume:

- The two-dimensional five fold ASTM to measure instantaneous concentration and velocity components at five different positions in the vertical direction.
- Two electromagnetic flow meters (EMF) arrayed vertically and mounted to the flume wall for velocity.
- Two optical back scatter sensors (OBS) for measurement of instantaneous concentration at two positions.
- A pump sampling system (10 intake nozzles) also located along the delta flume wall (intake nozzles at about 0.3 m from the wall).
- Ripple profiler to measure bed form: The Sand Ripple Profiler is a 2 MHz scanning sonar system comprising a pencil beam transducer on a rotating head. Thus for each head position a backscatter profile can be obtained, allowing a 2D image through the water to be built up. Data is transferred to a PC via serial link following capture using an on board 8 bit ADC.

Besides, other instruments were also used in this experiment. During the first test series this sand bed had a D_{50} of 0.33 mm, and during the second test series

the D_{50} was 0.16 mm. The ASTM frame was positioned on this sand bed. The water depth was 4.5 m in all experiments. The scheme for the positions of the measurement instrument is illustrated in Fig. 2.

According to the manufacturer (Delft Hydraulics) the error amount for measured velocity value is 10% and 30% for the measured concentrations.

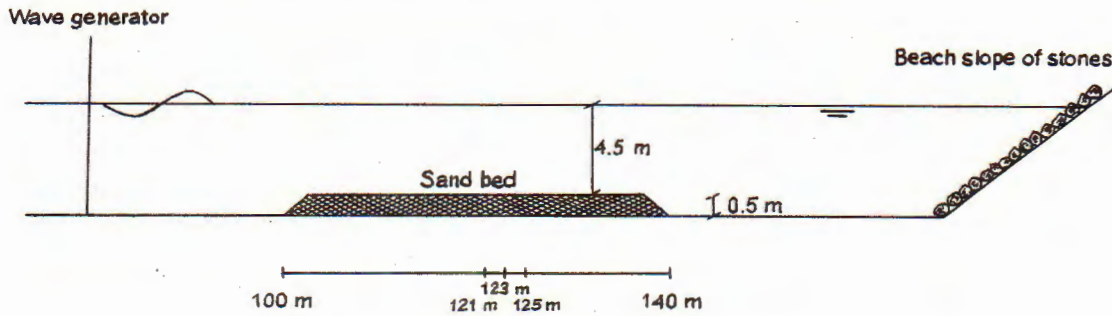


Fig. 1. Sketch of experimental set-up

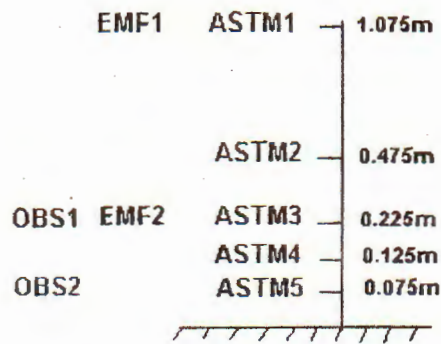


Fig. 2. Positions of instruments for measurement in the vertical direction

2.2. Experimental programme

The experimental conditions presented in Table 1 include different sand sizes, wave types, wave heights and the orientation of ASTM and they are divided into five groups. The orientation of the ASTM was changed during the test program in order to see the influence of measurement positions on the results. In this case the sensors are not located in the plane of orbital motion, so that the measurement volume is least disturbed by the sensors. However, in a field situation the direction of the waves cannot be controlled, which may lead to an unfavourable orientation of the ASTM with respect to the plane of orbital motion. The measurement levels above the bed for most tests are presented in Fig. 2. There are some special cases (D4, D5, E1, E2) for which the measurement levels were 0.175, 0.225, 0.325, 0.575 and 1.175 m.

Table 1. Measurement program

Data Set	Measurement No.	Number of test	Grain size d_{50} (mm)	Wave height Hs (m)	Orientation of ASTM (degree)
I	A1, A1B, A2A, D1, D2, D3, D4, D5	8	0.33	1.00	-90 -120
II	B1A, B2A, B1B, E1, E2, E3, E4, E5	8	0.33	1.25	-90 -120
III	G1, G2, G3, G4, J1, J2, J3	7	0.16	1.00	-120 -90
IV	H1, H2, H3, H4, H5, K1, K2, K3, K4	9	0.16	1.25	-120 -90
V	M1, M2, M4	3	0.16	1.50	-90

3. Experimental results

3.1. Distribution of suspended sand concentrations and velocities

In order to analyse the time series data from the experiment as well as from the field a software, namely TISERAT (Time Series Analysis Tool) has been developed with FORTRAN 90. Using this tool the instantaneous signal can be represented as the sum of time-averaged value and fluctuations for high and low frequencies as follows

$$c(z, t) = \bar{c} + \tilde{C}_s + \tilde{C}_\ell, \quad u(z, t) = \bar{u} + \tilde{U}_s + \tilde{U}_\ell, \quad v(z, t) = \bar{v} + \tilde{V}_s + \tilde{V}_\ell \quad (3.1)$$

in which $c(z, t)$, $u(z, t)$, $v(z, t)$ are instantaneous concentration and velocity components, respectively, the tilde sign “ $\tilde{\quad}$ ” denotes a fluctuation, the subscript s denotes high frequency fluctuation and ℓ for low frequencies and the overbar “ $\bar{\quad}$ ” denotes time-averaged values. The u -component is aligned along the long axis of the flume, positive in the onshore direction, and the v -component is aligned across the flume.

Typical vertical distributions of time-averaged concentration, cross-shore and longshore velocities are presented in Fig.3 for tests B2A and K2. It can be seen from these figures that the vertical distributions of time-averaged concentration show a well known behaviour, i.e. the concentration of sediment is very high near the bed and decreases monotonically towards the surface.

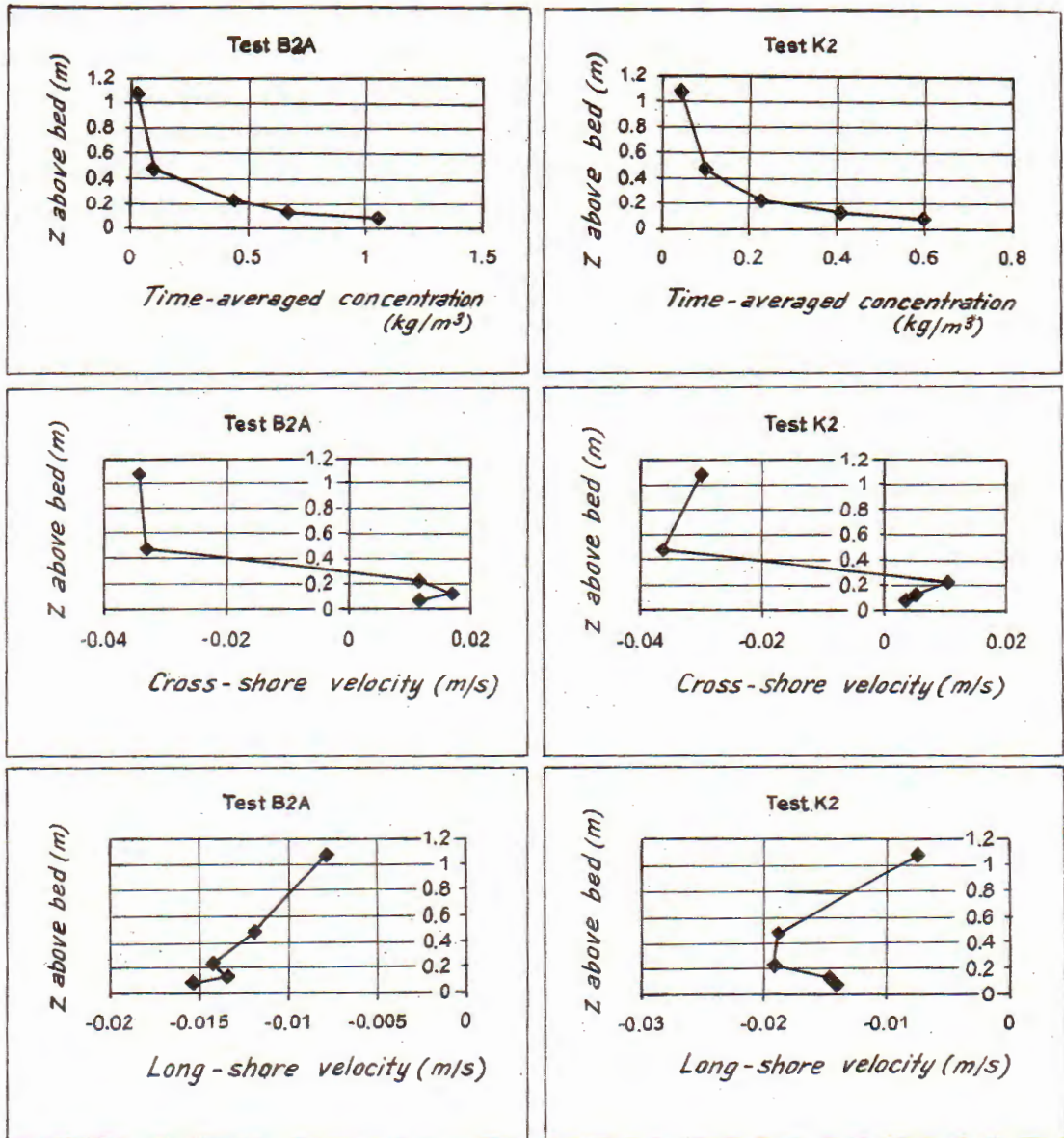


Fig. 3. Distribution of time-averaged concentrations and velocities

The range of time-averaged concentration at the highest elevation is from 0.01 g/l (test B1B) to 0.09 g/l (test M4) and the range at the lowest (number 5) is 0.32 g/l (test H4) - 1.38 g/l (test E4). Although sometimes in the field the sediment concentration may be higher than this, especially during a storm, the ranges of concentration that were created in the Delta flume are large enough to simulate most real cases.

The maximum cross-shore time-averaged velocities in onshore direction are 0.02 m/s at position number 3 (near the bed) for the test K1 and -0.04 m/s for

offshore at the position 2 of test H2. At the same time this value is also the maximum undertow velocity. The results of analysis of all the tests show that at the positions 1 and 2 the undertow currents always happen. This phenomenon is due to the influence of vertical circulation in the flume with onshore fluid flux between wave crest and wave trough and offshore return of fluid in the lower part of the water column. For long shore current the distribution of velocity has the same direction at the defined time point.

The tests G and J give the best time-averaged values in comparison with the other cases in standard deviation. This is easy to understand, because in the tests G and J the sand particle with $D_{50} = 0.16$ m, wave height is 1 m and especially the ripple height is small enough ($r = 0.03$ m) and the ripple length is quite long ($\lambda = 0.72$ m), yielding less variations in velocities and concentrations. Moreover, in some cases the duration of measurement is not long enough, such as 2 minutes for test B1B, 3 minutes for D4, 6 minutes for J3, 7 minutes for E2, H4 and 8 minutes for K3, M4.

3.2. Suspended sand transport components

3.2.1. Vertical distribution

Based on the definitions (3.1) the net suspended sediment transport rates in cross-shore and longshore directions are as follows

$$\begin{aligned}\overline{Q_x} &= \overline{u\bar{c}} + \overline{\tilde{U}_s\tilde{C}_s} + \overline{\tilde{U}_s\tilde{C}_\ell} + \overline{\tilde{U}_\ell\tilde{C}_s} + \overline{\tilde{U}_\ell\tilde{C}_\ell} \\ \overline{Q_y} &= \overline{v\bar{c}} + \overline{\tilde{V}_s\tilde{C}_s} + \overline{\tilde{V}_s\tilde{C}_\ell} + \overline{\tilde{V}_\ell\tilde{C}_s} + \overline{\tilde{V}_\ell\tilde{C}_\ell}\end{aligned}\quad (3.2)$$

in which the first terms of (3.2) are transport components relating to mean current, and the other terms relate to waves. This paper concentrates on the cross-shore processes, so the local longshore movement was not analysed in more detail.

The calculations of vertical distributions of sand transport components for all the tests are illustrated in Fig. 4. It shows that with five data sets the components of interaction between high and low frequencies are very small and can be ignored, while the components due to purely high and low frequencies are relatively large, so the omission of these components may cause a large error in the prediction computation.

At the elevations 1 (the highest above the bed) and 2 the undertow current always exists, so the time-averaged transport components corresponding to these elevations are always offshore directed. From the above results it is easily seen that the suspended sediment transport mainly occurs in the near-bed layer with a thickness of about 0.3 to 0.5 m, which is roughly equivalent to 10 to 20 times the ripple height.

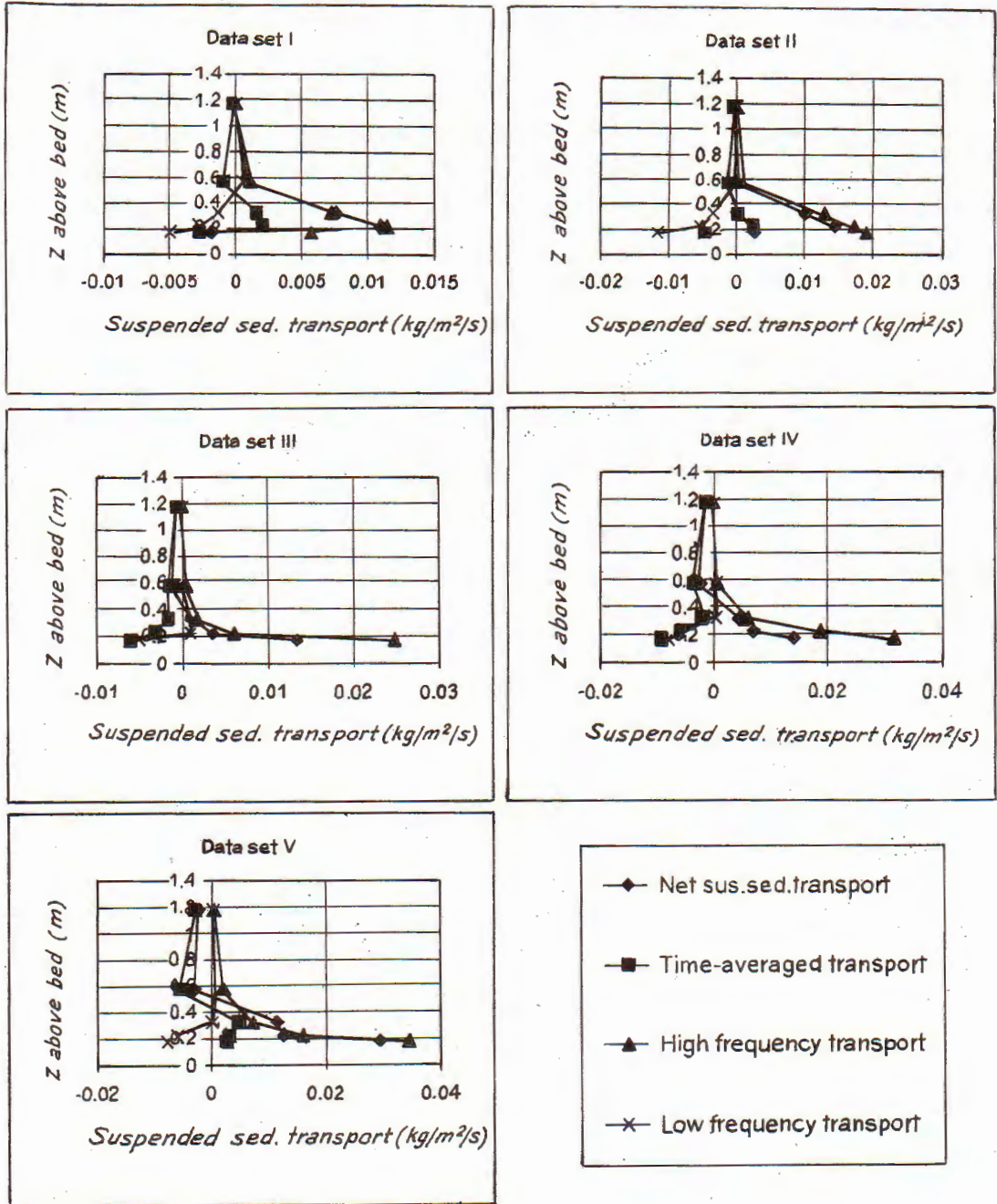


Fig. 4. Distribution of cross-shore sediment transport components for combined tests

3.2.2. Depth-integrated transport rates as a function of wave height

The relationship between sediment transport rates integrated over the depth

and wave height is presented in Fig.5 based on the calculations for 35 tests of irregular waves. It shows that the time-averaged suspended sediment transport rates are in the offshore direction, while the suspended sediment transport rates for high frequency go together in the same direction of wave propagation in the onshore. These remarks are similar with those of previous studies, such as Vincent and Green, 1990; Osborne and Greenwood, 1992; Osborne and Vincent, 1996; Grasmeyer and Van Rijn, 1999, Van Rijn et al., 1993 and Van Rijn, 1998. At the same time the results also show that the significant wave height plays an important role in transport rates, which increase according to the growth of wave height. The influence of particle diameter is also seen clearly. Under the action of waves, coarser sand particles are brought further toward the land and the mean current brings the finer sand in the opposite direction. Note that the standard deviations due to averaging tests of the same conditions on wave and grain size are quite large because of the local influence of ripples.

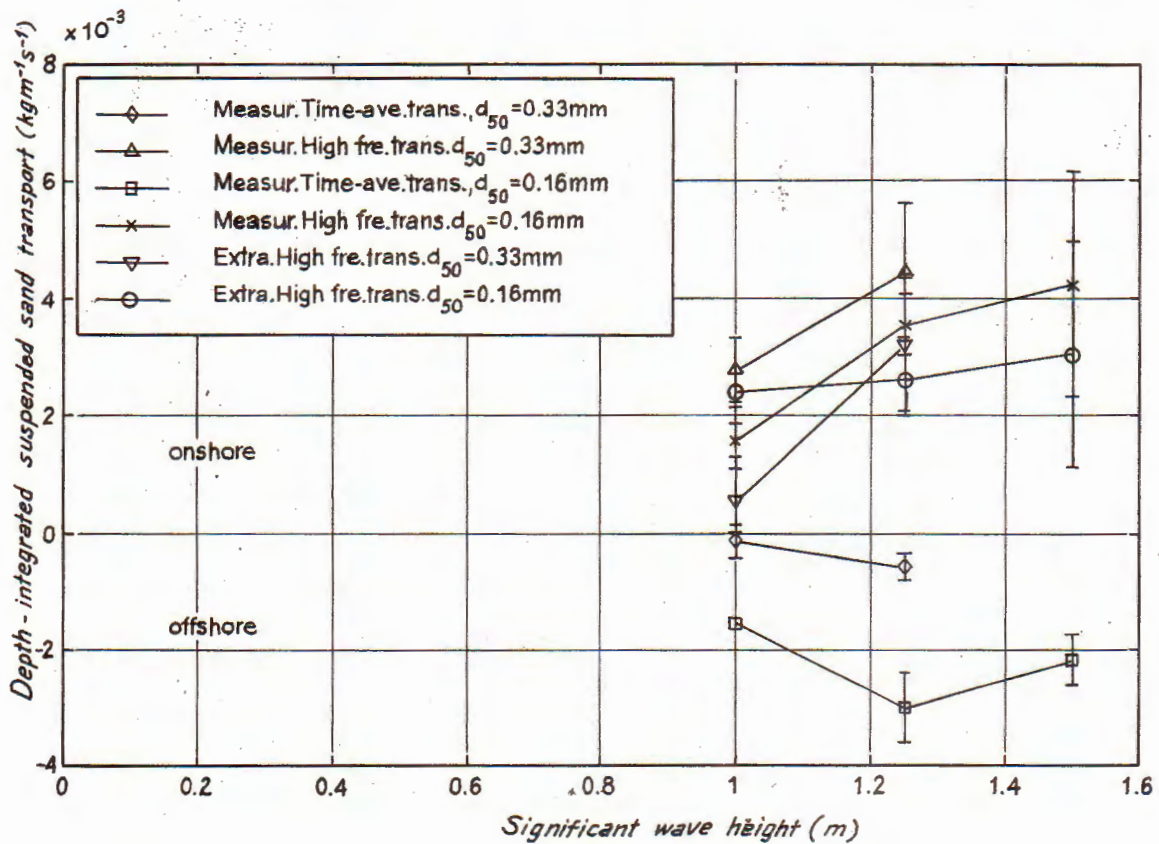


Fig. 5. Relationship between the significant wave height and depth-integrated transport

4. Prediction of wave related suspended sand transport (high frequency)

4.1. Houwman's method

Houwman and Ruessink (1996) found that the high-frequency suspended sediment transport plays an important role in the net transport and cannot be neglected. In their approach the mean sediment concentration at a certain height above the bed is thought to be the time-averaged value of two sediment concentration peaks per wave cycle, one during the onshore directed wave motion and the other during the offshore directed wave motion. According to the velocity moments approach the shape of the sediment concentration peaks can be assumed to be equal to the shape of $|u(t)|^3$. If it is also assumed that each half wave cycle can be described with the linear wave theory with different amplitudes but with equal duration it follows

$$\bar{c}(z) = k(U_{on}^3 + U_{off}^3) \frac{2}{T} \int_0^{T/2} \sin^3 \omega t dt \quad (4.1)$$

In equation (4.1), the left term is the time-averaged sediment concentration at height z above the bed, U_{on} and U_{off} refer to the onshore and offshore peak orbital velocity, T and ω are the wave period and angular frequency respectively and k is a constant.

The oscillatory suspended sediment transport at a certain height z above the bed can be related to the fourth order moment $u \cdot |u^3|$. The wave-averaged oscillatory sediment transport rate $Q(z)$ through a layer dz is then described by:

$$Q(z) = k' \bar{c}(z) \frac{U_{on}^4 - U_{off}^4}{U_{on}^3 + U_{off}^3} dz \quad (4.2)$$

$$k' = \frac{1}{2} \int_0^{T/2} \sin^4 \omega t dt \left(\int_0^{T/2} \sin^3 \omega t dt \right)^{-1} \approx 0.441786 \quad (4.3)$$

Figure 6 shows the comparison of this expression with measurements, indicating that the Houwman formula tends to overestimate the measured values.

However, by replacing the coefficient k' in Houwman's formula the result becomes much better as will be seen below.

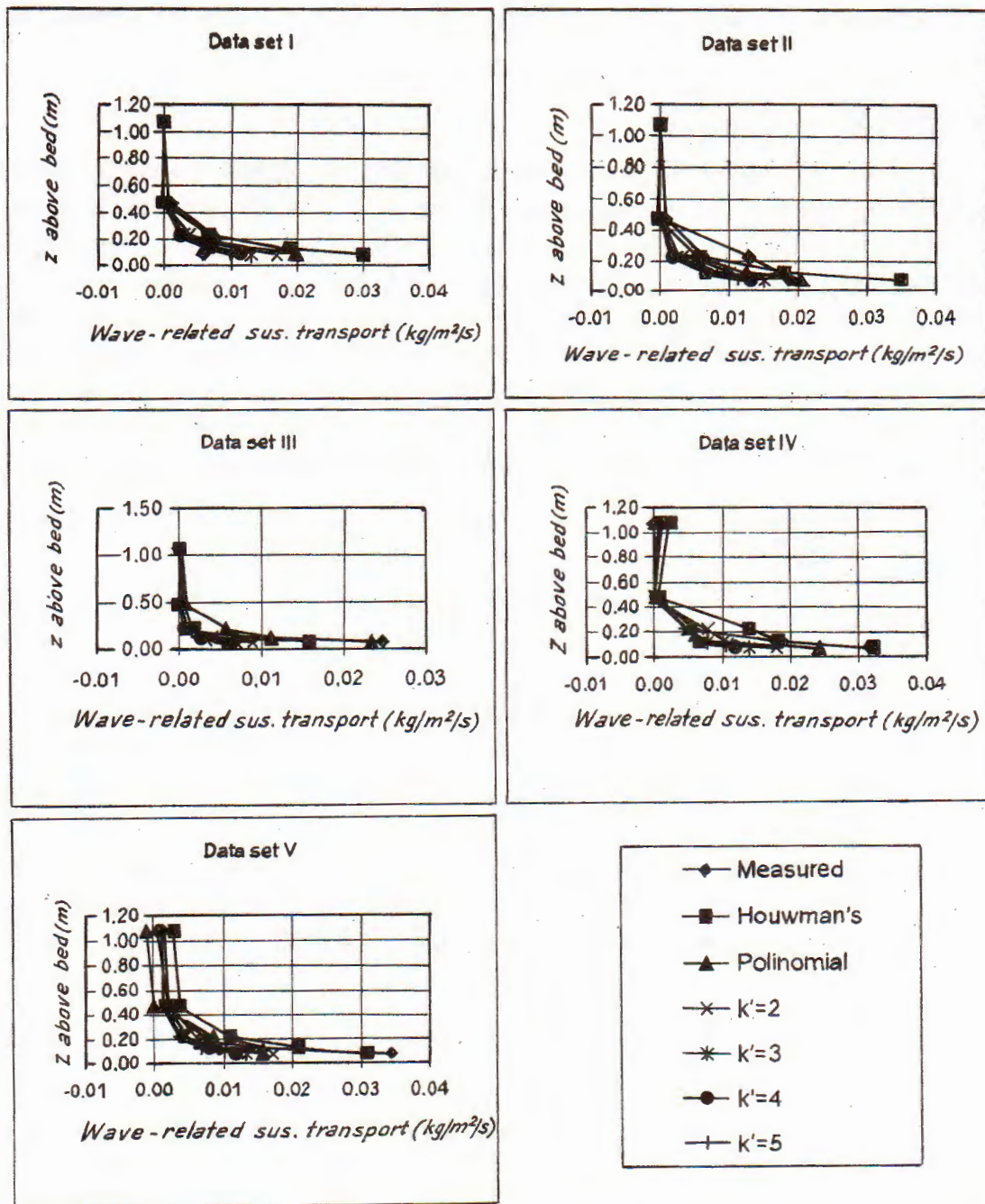


Fig. 6. Comparison between measured and predicted wave-related suspended transports

4.2. The proposed methods

4.2.1. Polynomial of degree 3

Based on the tests that were carried out from the Delta flume, the polynomials of degree 3 by the least-squared method were derived. This method is found to

be quite suitable and convenient for computations of the total and high frequency cross-shore transport rates. Therefore, for each transport rate a set of 5 polynomials of degree 3 were established at 5 given different elevations above the bed, as illustrated in Figure 2.

- The polynomials for the total transport rates at 5 elevations:

$$\begin{aligned}
 P_1(x_1) &= -68881.681223x_1^3 - 759.7258128x_1^2 - 0.307980x_1 - 0.000246 \\
 P_2(x_2) &= -1406.106594x_2^3 - 16.489452x_2^2 + 1.179563x_2 + 0.001532 \\
 P_3(x_3) &= -582.838108x_3^3 - 22.231484x_3^2 + 1.450788x_3 + 0.005621 \\
 P_4(x_4) &= 398.955682x_4^3 + 18.650784x_4^2 + 0.963271x_4 + 0.008338 \\
 P_5(x_5) &= -19.328564x_5^3 - 11.071669x_5^2 + 0.384421x_5 + 0.012661
 \end{aligned} \tag{4.4}$$

- The polynomials for high frequency transport rates at 5 elevations:

$$\begin{aligned}
 P_{s1}(x_1) &= -51668.624053x_1^3 - 628.676562x_1^2 - 1.110219x_1 - 0.000255 \\
 P_{s2}(x_2) &= -454.081467x_2^3 + 5.420804x_2^2 + 0.270642x_2 + 0.001277 \\
 P_{s3}(x_3) &= -626.606571x_3^3 - 22.193335x_3^2 + 0.544458x_3 + 0.006672 \\
 P_{s4}(x_4) &= 438.404485x_4^3 + 23.969238x_4^2 + 0.191164x_4 + 0.011455 \\
 P_{s5}(x_5) &= -47.133831x_5^3 - 18.305949x_5^2 - 0.928461x_5 + 0.018469
 \end{aligned} \tag{4.5}$$

in which x_i , P_i , P_{si} ($i = 1, 2, \dots, 5$) are the time-averaged, net cross-shore transport rates, and high frequency transport rates respectively, corresponding to 5 measurement elevations in the vertical direction.

The results of computation based on this method for the high frequency cross-shore transport rates are presented in Figure 6. With the absolute error value of 10^{-3} this method has most tests that satisfied the given standard. At the same time from Figure 6 it is seen that the curve based on this method fits quite well with the measurement.

4.2.2. Modified Houwman's method

As mentioned above, this method is used to modify the Houwman's method by introducing the power n for concentration instead of a fixed power 3 and by choosing the optimum coefficient k' from many different values on the basis of comparison with the computed results for 35 tests of irregular waves. Relative and RMS (root mean square) errors are used as the standards to evaluate the errors instead of absolute error standard, because sometimes the local differences between measurement and computation are very large. So, by this way the modified Houwman's formula to compute the high frequency cross-shore suspended

sediment transport rate at elevation z above the bed, is as follows

$$Q_{shm} = k' \bar{c} \frac{U_{on}^{n+1} - U_{off}^{n+1}}{U_{on}^n + U_{off}^n} \quad (4.6)$$

in which U_{on} is defined as the mean of peak onshore velocities by 33% of the highest values, similarly U_{off} is from 33% of peak offshore velocities. The coefficient k' will be determined for each value of n ($n = 2, 3, 4$ and 5) so that the minimum RMS error is achieved:

$$\min_{1 \leq j \leq 700} (A_n), \quad n = 2, 3, 4, 5 \quad (4.7)$$

$$A_n = \left(\frac{1}{N \max_i (Q_{sszdi}^2)} \sum_{i=1}^N (Q_{sszdi} - Q_{shmdi})^2 \right)^{1/2} \quad (4.8)$$

or

$$A_n = \max_{1 \leq i \leq N} |(Q_{sszdi} - Q_{shmdi}) / Q_{sszdi}|, \quad (4.9)$$

in which A_n is a measure of the difference between the predictions and the measurements, $N = 35$ or 48 (number of tests); Q_{sszdi} , Q_{shmdi} are depth-integrated high frequency cross-shore suspended sediment transport rates by calculating the i th measured data and by using the formula (4.6), respectively; the subscript j denotes the number of step that the coefficient is decreasing from a initial value of 0.8 in this report.

Finally, the best values for k' with the minimum RMS error and the lowest maximum of relative errors for 4 cases of the power n are obtained as follows

- $k' = 0.247$ for $n = 2$
- $k' = 0.193$ for $n = 3$
- $k' = 0.166$ for $n = 4$
- $k' = 0.145$ for $n = 5$

The results of computations for these values of k' are also illustrated in Figure 6. It shows that the case of $n = 2$ is better, because the maximum of relative error from comparison with 48 tests is approximately 250%, e.g. the maximum absolute error is about 2.5 times the measurement, while for the other cases of n the maximums of relative errors are more than 250%. The case of $n = 5$ gives maximum relative error larger than other cases. The minimums of RMS errors are not much different for 4 cases of n .

However, these values of k' are only based on a concrete set of measurement data (35 tests of irregular waves), so they are not unique values. In order to

get a high accuracy, a comparison with measurement is necessary to adjust this coefficient. In general, the range of k' from 0.14 to 0.25 are able to be used. Furthermore, this coefficient is likely to depend on parameters of bed form, fluid dynamics and the physical nature of sediment particles, so calibration is necessary.

The obtained results show that the different values of power n have little influence on the accuracy, provided that a suitable coefficient is chosen.

5. Bedload transport

So far the instrument to measure instantaneous bedload transport is not available. Therefore, extrapolation is necessary for calculation of suspended sediment transport between $z = 0.075$ m and 0.01 m and an experimental formula based on instantaneous velocity is used to estimate the bed load transport (Van Rijn, 1998), namely

$$\frac{q_b}{\sqrt{(s-1)gD_{50}^2}} = m(|\theta'| - \theta'_{cr})^n \text{sign}(\theta') \quad (5.1)$$

in which q_b is the instantaneous transport rate during the wave cycle ($m^3/m/s$), s relative density of sediment, ρ , ρ_s densities of water and sediment (kg/m^3), g acceleration due to gravity (m/s^2), D_{50} median grain size of sediment (m), m , n coefficients, θ' instantaneous dimensionless bed shear stress and θ'_{cr} critical dimensionless bed shear stress known as the Shields parameter.

The instantaneous dimensionless bed shear stress is calculated by the following formula:

$$\theta' = \frac{\tau'}{(\rho_s - \rho)gD_{50}}, \quad (5.2)$$

with

$$\tau' = \frac{1}{2}\rho f_{cw}u|u|, \quad f_{cw} = \alpha f_c + (1 - \alpha)f_w, \quad \alpha = \frac{|u_a|}{|u_a| + \hat{U}_\delta},$$

$$\hat{U}_\delta = \begin{cases} \frac{1}{2}(U_{on} + U_{off}) & \text{in case of irregular waves} \\ \hat{U} & \text{in case of regular waves} \end{cases}$$

$$f_c = 0.24 \left(\log\left(\frac{12h}{k_{sc}}\right) \right)^{-2}, \quad f_w = \exp\left(-6 + 5.2\left(\frac{\hat{A}_\delta}{k_{sw}}\right)^{-0.19}\right)$$

$$\hat{A}_\delta = \left(\frac{T}{2\pi}\right)\hat{U}_\delta, \quad k_{sc} = k_{sw} = 3D_{90}, \quad f_{w,max} = 0.3$$

in which α is weighted coefficient; τ' -bed shear stress; u_a -time-averaged cross-shore velocity; f_c and f_w -friction factors related to current and wave, respectively; u -instantaneous cross-shore velocity (m/s); \hat{A}_δ -near-bed peak orbital excursion (m);

k_{sc} , k_{sw} friction factors related to current and wave(m), respectively; \hat{U} -amplitude of horizontal (sinusoidal) velocity (m/s).

In order to calculate the bedload transport for high frequency, the instantaneous velocity u is replaced by high frequency cross-shore velocity in the above formulae.

From the results it is seen that the scales of suspended sediment transports are greater than the scales of bedload transports. At the same time it also shows that the bedload transport based on instantaneous velocity is dominant to high frequency bedload transport. About the movement direction, in general, net bedload transport is almost in an offshore direction, while high frequency bedload transport almost moves to an onshore direction together with high frequency suspended sediment transport.

6. Evaluation on relative importance of transport components in three layers

In order to have a general evaluation of total sediment transport rates over the water depth, calculations for transport components at three layers are required. The transport rate in layer 1 is obtained from measurement, layer 2 is from extrapolation and layer 3 is predicted by bedload transport and they are presented in Figure 7 for a significant wave height of 1m and in Figure 8 a for a wave height of 1.25m. From the obtained results it can be observed that sediment transport rates increase in all three layers for coarse and fine sand when the wave height increases. This comment is a generalisation of the one in section 3.2.2 for three layers. The figures show that the scales of sediment transport rates at layers 2 and 3 for high frequency are not small and cannot be ignored. The contribution of layer 2 (extrapolation) is about 20-30% of the total sediment transport rate and the contribution of layer 3 (bedload) is about 15-20%. The extrapolation does not have a very high reliability, but at least it also gives some suggestion for the measurement in the field work, by confirming that sediment transport near bed occupied a significant part of the total transport. Figures 7-8 appear to indicate that under waves, the bigger grain size is easily kept in suspension, while the ratio of bedload transport is almost unchanged according to different grain size. However, only two particle sizes are tested, so it is difficult to give a strict conclusion on the influence of particle size on the behaviour of suspended sediment and bedload transport.

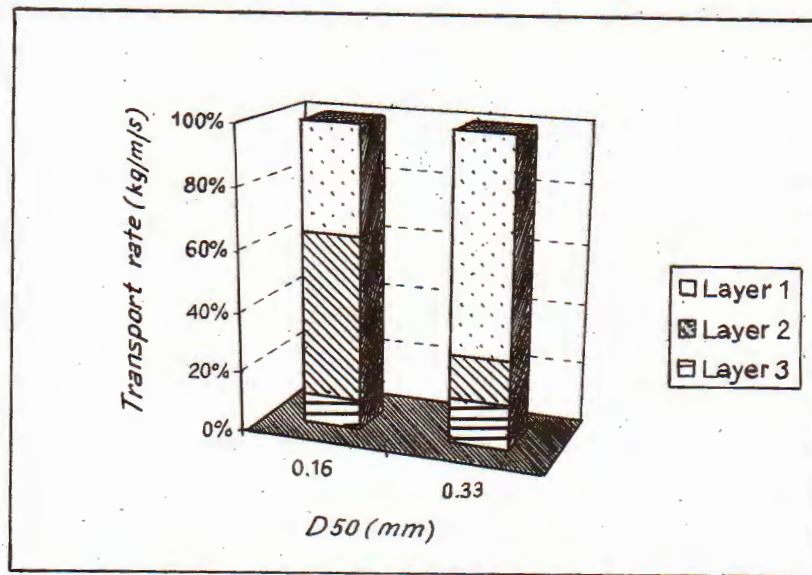


Fig. 7. Representation of relationship between high frequency transport rate and particle size in 3 layers when significant wave height $H_s = 1$ m

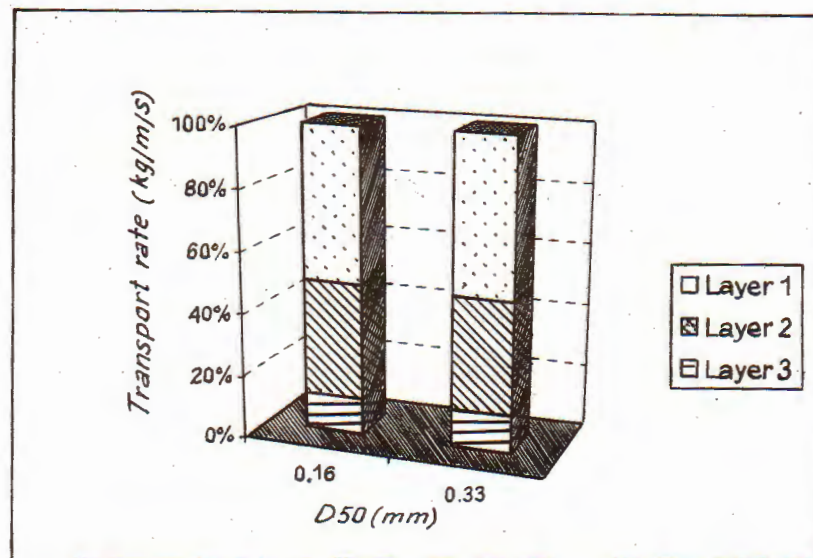


Fig. 8. Representation of relationship between high frequency transport rate and particle size in 3 layers when significant wave height $H_s = 1.25$ m

7. Conclusions and recommendations

From the above results, the following conclusions can be drawn:

- The sediment transport components related to the wave and current usually have opposite directions. The results of the analysis show that the time-averaged transport rates are mostly offshore directed, while the high frequency transport rates have a trend towards an onshore direction. So which term of transport rate as well as which direction is more important should be considered carefully.
- The transport component due to pure high frequency sometimes becomes more significant in comparison with the transport term of mean current. Therefore, the omission of this transport term in evaluating the process of sand transport may cause serious error.
- In all tests considered, the undertow current always exist. This phenomenon is related to onshore mass transport between the wave crest and wave trough, which is compensated by an offshore return current below the wave trough in a straight flume.
- The factors of wave height and size of particle also play an important role in transport rate. The transport rate increases when wave height becomes larger. The role of particle size is quite clear for high frequency suspended sediment transport in layer 2 between $z = 0.01$ m and $z = 0.075$ m. In general, the transport rate in this layer increases when the particle size and wave height become smaller. In the other layers, the influence of particle size on the behaviour of transport rate is not very clear.
- In order to get more accurate evaluation on the transport rate the number of measurement elevations close to the bed (first measurement level at about 0.02 m above bed) should be increased, so that the depth-integrated transport rate can be determined with sufficient accuracy.
- To evaluate the relative importance of sediment transport in three layers, the procedure of extrapolation may be necessary. However, extrapolation should be done at the elevations very close to measurement points, otherwise it will give a very large error. In general, the three methods of extrapolation that are mentioned in this report, can be used.
- For Houwman's and Dang's methods, the calculation of suspended sediment transport is quite simple and easy and extrapolation should be implemented directly from known values, instead of extrapolating the variables of the functions. However, Dang's method is only suitable for conditions similar to those carried out in Delta flume (present data set), otherwise it may give a larger error. It should also be noted that the least squared method needs to be reapplied to a new data set to obtain new polynomials.

- The bedload transport cannot be measured directly, but it can be estimated by bedload transport formula using instantaneous total velocity. It may have a dominant role in comparison with suspended sediment transport and has the trend of offshore movement, while high frequency bedload transport is the opposite.

Acknowledgement

This publication is completed with financial support from the National Basic Research Program in Natural Sciences.

This paper is also a part of work carried out in the frame of the Scholarship program of Utrecht University that the author has been awarded. He would like to take this opportunity to express his deep gratitude to Prof. Dr. Leo C. Van Rijn for his very useful remarks, especially for his very kind interest and assistance.

REFERENCES

1. Dang Huu C. and Grasmeijer B. T. Analysis of sand transport under regular and irregular waves in large-scale wave flume. Report R99-05, IMAU, Utrecht University, The Netherlands 1999.
2. Dang Huu C., Leo C. Van Rijn and Grasmeijer B. T. Wave-related suspended sand transport under irregular waves in the ripple regime. International Conference on Coastal Engineering, Sydney, 2000 (accepted)
3. Grasmeijer B. T. Dang Huu C. and L. C. van Rijn, Depth-integrated sand transport in the surf zone. Coastal Sediment'99, New York, Vol. 1, 1999, pp. 325-340.
4. Grasmeijer B. T. and L. C. van Rijn, Transport of fine sands by currents and waves, part III: breaking waves. Journal of Waterway, Port, Coastal, and Ocean Engineering, 1999. (Accepted for publication March 1999)
5. Houwman K. T. and B. G. Ruessink. Sediment transport in the vicinity of the shoreface nourishment of Terschelling. Proc. of the 25th International conference "Coastal Engineering 1996", Florida, Sep. 2-6, 1996, pp. 4793-4806.
6. Osborne P. D. and Greenwood B. G. Frequency-dependent cross-shore suspended sediment transport 2: A barred shoreface. Marine geology 106, 1992, pp. 25-51.
7. Osborne P. D. and Vincent C. E. Vertical and horizontal structure in suspended sand concentrations and wave-induced fluxes over bed forms. Marine

- Geology 131, 1996, pp. 195-208.
8. Ribberink J. S. Bed-load transport for steady flows and unsteady oscillatory flows. Coastal Engineering 34, 1998, pp. 59-82.
 9. Van Rijn L. C. Principles of sediment transport in rivers, estuaries and coastal seas, Aqua Publications, Amsterdam, The Netherlands, 1993.
 10. Van Rijn L. C. et al. Transport of fine sands by currents and waves I. Journal of Waterway, Port, Coastal and ocean Engineering, Vol. 119, No 2 , 1993, pp. 123-143.
 11. Van Rijn L. C. Principles of coastal morphology. Aqua Publications, Amsterdam, The Netherlands, 1998, p. 750.
 12. Van Rijn L. C. and Havinga F. J. Transport of fine sands by currents and waves II. Journal of Waterway, Port, Coastal and ocean Engineering, Vol. 121, No 2, 1995, pp. 123-133.
 13. Vincent C. E. and Green M. O. Field measurements of the suspended sand concentration profiles and fluxes and of the resuspension coefficient over a rippled bed. Journal of Geophysical Research Vol. 95 (C7), 1990, pp. 11591-11601.

Received December 15, 1999

MỘT VÀI KẾT QUẢ THÍ NGHIỆM VỀ VẬN CHUYỂN BÙN CÁT
DƯỚI TÁC ĐỘNG CỦA SÓNG TRONG MÁNG SÓNG LỚN

Bài báo trình bày một vài kết quả nghiên cứu trên máng sóng cỡ lớn của Delft Hydraulics. Sự phân tích chuỗi số liệu phụ thuộc thời gian của nồng độ bùn cát và vận tốc đã được tiến hành đối với sóng đều và không đều với các điều kiện khác nhau về sóng và cỡ hạt. Từ các giá trị được đo của nồng độ và vận tốc các thành phần tốc độ tải lơ lửng được tính và đã thu nhận được một số thông tin thú vị. Đồng thời một vài công thức bán thực nghiệm về tốc độ tải toàn phần trên cơ sở giá trị được đo, giá trị nội suy và công thức dự báo bùn cát đáy.

Institute of Mechanics, 264 Doi Can, Hanoi, Vietnam

Fax: 84-4-8333039, Email: Dhchung@im01.ac.vn